

# BENCHMARK TESTING FOR SPACEBORNE GLOBAL POSITIONING SYSTEM RECEIVERS

Greg N. Holt\*

*The University of Texas at Austin  
Austin, TX*

E. Glenn Lightsey†

*The University of Texas at Austin  
Austin, TX*

and Oliver Montenbruck‡

*DLR German Space Operations Center  
Oberpfaffenhofen, Germany*

The use of spaceborne Global Positioning System (GPS) receivers has increased as space mission designers seek to obtain high quality navigation and science data. Receiver selection is often complicated, however, by specific mission requirements and non-uniform manufacturer testing standards. A uniform set of benchmark tests was defined by which receivers may be independently evaluated for a variety of space mission requirements. In addition, a subset of these tests was performed and documented. The receivers used for this study included the Mitel Architect, Zarlink Orion, Goddard Space Flight Center PiVoT, Jet Propulsion Laboratory BlackJack, Trimble Force-19, Johnson Space Center Ship Channel, Surrey SGR-20, Asthech G12, and NovAtel Millenium. This study sought to characterize the raw measurement accuracy and tracking loop errors by using a GPS constellation simulator. To this end, a differencing technique was introduced which preserves systematic errors in the solution. The results of this study showed correctable systematic errors in two of the receivers which were tested. Raw measurement accuracy was also verified for all the tested receiver models.

## INTRODUCTION

**I**N recent years, the Global Positioning System (GPS) has become a common sensor for spacecraft navigation and, in some cases, attitude determination. The primary means for evaluating candidate GPS receivers for mission requirements has traditionally been through the use of manufacturer supplied documentation, such as performance specifications. However, these receiver performance results are not standard and may not be reproducible. Also, receivers are rarely tested under similar conditions, so that their results may be compared. As more mission planners turn to GPS to meet their navigation requirements, the need for an independent evaluation of receiver performance becomes apparent.

This study defines a standard set of tests that may be used to characterize spaceborne GPS receivers. These tests provide mission planners with important information on the inherent accuracy and tracking loop performance of GPS receivers that may be considered for use on their spacecraft. For this study, a

subset of tests was carried out on a group of nine GPS receivers. These results are documented and discussed.

Previous studies in this area include Montenbruck & Holt<sup>1</sup> and Williams et al.<sup>2</sup> Both of these papers discuss a similar test regimen on a single receiver design. This study expands substantially on the previous work by sampling a large number of receiver designs and directly comparing the results.

Receiver performance may be defined on many levels, most obviously the final processed navigation solution. This solution, however, is heavily dependent on the estimation and filtering of the raw measurements and will vary by application. More fundamentally, the receiver performance may be characterized by raw measurement accuracy and systematic tracking loop errors. These low-level performance measurements are common to the entire GPS architecture and are the focus of this study. Any navigation algorithm written for a particular application will be fundamentally limited by the accuracy of the raw measurements from the receiver. In addition, evaluating the raw measurement performance is useful to understand and optimize the low-level receiver software.

In order to provide full insight into the characteristics of the tracking loops and measurement collection,

\*AIAA Student Member (SS), Doctoral Student

†AIAA Senior Member (SH), Assistant Professor

‡Head GPS Technology & Navigation Group

all errors must be preserved, isolated, and reported in the analysis. For this reason it is necessary to perform the raw measurement and tracking loop evaluations on a GPS constellation simulator. Although a stationary outdoor antenna is much less expensive and more accessible for most testers, it has several drawbacks when compared to a simulator. The constellation simulator is able to provide a realistic high Doppler environment which affects the raw measurements in space but is not seen in a ground test. The simulator is also able to provide an environment free from external errors such as satellite ephemeris errors, satellite clock errors, ionosphere and troposphere effects, and multipath. Any errors seen in the simulation tests are primarily due to the receiver hardware and tracking loops. Simulators are also able to create repeatable test conditions which lead to verifiable results.

## BENCHMARK TESTING AND SCOPE

GPS receiver benchmark testing is a wide field with many aspects and procedures. This section gives an overview of the different types of benchmark testing, then defines the subset of tests actually performed for this analysis.

### Test Types

Each of the following test types is a part of the overall benchmark evaluation of a spaceborne GPS receiver. These tests are summarized in the test matrix of Figure 1 with priorities assigned based on the relevance of the tests for a given application.

#### Static

A static test is simple to perform and gives basic information on receiver performance. Static tests may be performed with live-sky measurements or in simulation (with and without external errors). If live-sky and simulated data is compared, receiver error tolerance may be observed. This test does not simulate the high Doppler environment of space flight, however, so the tracking loop performance will not be comparable to that of an orbital environment.

#### On-Orbit

Short of actual space flight test opportunities (e.g., sounding rockets), an on-orbit test is only available in simulation. A spaceborne GPS system, however, will spend most of its operational life performing on-orbit navigation. This high Doppler environment will affect the receiver tracking loops differently than a static scenario. For this reason, an on-orbit evaluation is a high priority test when validating or selecting a receiver design. On-orbit tests may be used with environmental and ephemeris errors disabled to evaluate raw measurement accuracy and tracking loop performance. These simulations may be conducted for various orbit and mission types. The polar, LEO (Low Earth Orbit)

	Priority 2		Priority 1				Priority 3			Priority 4		Priority 5		
	Static	Live-Sky Simulated	Error Free	Perturbations	On Orbit Sounding Rocket Simulator	LEO	polar station	GEO	PL	Hardwire Baseline	Zero Fixed	Dynamic	Orbital ReilNav Error	Error-Free Integrated
Code Accuracy	X	X	X	X	X	X	X	X	X	X	X	X	X	X
Carrier Accuracy	X	X	X	X	X	X	X	X	X	X	X	X	X	X
Range-Rate Accuracy	X	X	X	X	X	X	X	X	X	X	X	X	X	X
Tracking Loop Errors				X	X	X	X	X	X	X	X	X	X	X
Error Sensitivity					X	X	X	X	X	X	X	X	X	X
Pseudolite Performance									X	X	X	X	X	X
Integrated Performance														X

**Fig. 1 Benchmark Test Matrix**

on-orbit subset of tests was selected and performed for this study. The polar test produces a high variation of satellite visibility and Doppler shifts for evaluating raw measurement accuracy and tracking loop performance.

#### Pseudolite

Pseudolites (GPS signal transmitters) have gained interest for their abilities in close proximity spacecraft rendezvous (e.g., near the International Space Station). A spaceborne GPS receiver used in this situation will need special firmware modifications to effectively receive, process, and utilize these pseudolite signals. Receivers with this capability may be tested initially by wiring directly to a pseudolite. In later test phases, a pseudolite constellation may be used in a variety of noise environments with static and dynamic antenna motion. More information concerning pseudolites may be found in Stone.<sup>3</sup>

#### Orbital Relative Navigation

For receiver applications where relative navigation is anticipated, a simulated orbital test is useful to evaluate receiver performance and navigation filter design. In general, two receivers are needed and a real time loop is established to accomplish the relative navigation. By using both error and error-free scenarios, a filter sensitivity may be estimated and compared with other filter/receiver combinations.

#### Integrated

Much interest has been expressed in combining a GPS system with other sensors such as an Inertial Navigation System (INS) or star tracker to provide better navigation quality than either sensor could alone. These integrated systems can be tested in simulation, but simulated secondary sensor measurements must be provided in addition to a GPS simulator in order to stimulate both systems. This test will generally only be necessary if anticipated uses of the GPS receiver include integrated systems.

#### Test Matrix

The test matrix for GPS receiver benchmark characterization is shown in Figure 1. This matrix shows which set of tests supply information about which as-

pects of receiver performance. Each column of the test matrix represents a receiver characteristic to be evaluated. Code, carrier, and range rate accuracy are related to the raw measurement performance of the receiver. Tracking loop errors are related to the firmware design. Error Sensitivity is evaluated by comparing receiver performance with and without environmental and ephemeris errors. The Pseudolite and Integrated categories are related to the receiver performance in these specialized environments. Attitude determination from a GPS receiver is related to the carrier phase measurement and is covered by that test.

### Scope

To completely evaluate the performance of a receiver, the entire test matrix should be considered. For this study, however, only a portion was completed as time allowed. In Figure 1 the scope of this project is highlighted in the overall test matrix. A near polar LEO scenario provides useful information about the phase of operation where a spaceborne receiver spends most of its operational lifetime. Even though the simulation is for a polar orbit, these results may be transferred to other inclinations since a polar orbit will produce the highest variation of satellite visibility and Doppler shift and other orbits may be considered to be less extreme examples of that case.

## TEST CONFIGURATION

The constellation simulator used for this research is shown in Figure 2(a). It is a Spirent (formerly Global Simulation Systems) model STR4760 and has 2 dual-frequency output ports with 16 channels per port. Complete simulator specifications may be found in the manual by Spirent.<sup>4</sup> The simulator is controlled by a Digital Electronics Corporation (DEC) Alpha Workstation shown in Figure 2(a). It is manufactured by Compaq, Inc. and uses the Open Virtual Memory System (Open VMS) operating system.

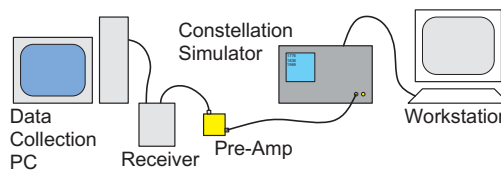
A complete description of the orbital simulation scenario is found in Holt.<sup>5</sup> The scenario is summarized below.

- Semi-major Axis: 6823.0 km
- Eccentricity: 0.001
- Inclination:  $87^\circ$
- Longitude of Ascending Node:  $135^\circ$
- Argument of Perigee:  $0^\circ$
- Mean Anomaly:  $0^\circ$
- Epoch: 6 Nov 2001 00:00.00 GPS, 5 Nov 2001 23:59:57 UTC
- GPS Week: 1139, 172800 seconds

The orbital simulation is for a low earth satellite in a near polar orbit. The almanac file used to generate this scenario was YUMA1139. All environmental and ephemeris errors were eliminated from this scenario. These include ionosphere, troposphere, multipath, satellite clock, and satellite ephemeris errors.



a) GSSi GPS Constellation Simulator and DEC Alpha Open VMS Workstation



b) Test Setup

Fig. 2 Laboratory Simulation Equipment

For this experiment the components were set up in the configuration of Figure 2(b). The standard orbital test was initiated on the simulator during each data run. The signal was sent through a preamplifier and then to the receiver under evaluation, with the signal gain adjusted for the operating level of each individual receiver. The data output stream was collected on a Personal Computer (PC) via a serial connection. Each receiver was tested for two hours in this environment. This time span was sufficient to give multiple horizon to horizon GPS visibility arcs for differencing.

Each receiver in the test had unique hardware and software components which affected its performance. Most receivers had 12 channels, but some had as few as six. For tracking loops, different combinations of phase lock loops (PLL) and frequency lock loops (FLL) were used. Most receivers use a temperature controlled crystal oscillator (TCXO), but the Blackjack uses a steered voltage controlled crystal oscillator (VCXO). Several receivers also had multiple Radio Frequency (RF) ports, front ends, and correlators for multiple antenna attitude determination.

### Architect

The Architect receiver was manufactured by Mitel Semiconductor (presently Zarlink Semiconductor). It is based on the Plessey chipset using the ARM32 microprocessor and is user programmable with available source code. The Architect receiver was originally designed for terrestrial applications as a 12-channel, single frequency, single RF design. Source code modifications by GSOC have made the receiver capable of outputting code, carrier, Doppler offset, carrier smoothed code, and carrier derived range-rate. This source code has internal time tag synchronization to integer seconds on GPS Time when position fixing. The modified firmware uses a second order FLL-aided PLL for its tracking loop. The receiver hardware in-

cludes a TCXO and GP2021 correlator. The Architect has no space flight history as it was designed only as a development tool for GPS receiver research. Complete documentation for the Architect receiver may be found in the manual by Mitel.<sup>6</sup>

### Orion

The Orion receiver is based on a published design by Zarlink using the Plessey chipset and produced by Deutsches Zentrum für Luft-und Raumfahrt (DLR). The test model was built at the German Space Operations Center (GSOC) and the source code was refined at The University of Texas at Austin Center for Space Research. Like the Architect, the Orion receiver was originally designed for terrestrial applications as a single frequency, 12 channel, single RF design. DLR source code modifications have made the receiver capable of outputting code, carrier, Doppler offset, carrier-smoothed code, and carrier-derived range rate measurements. This source code has internal time tag synchronization to integer seconds based on GPS Time when position fixing. The DLR firmware used in this test uses a second order FLL-aided PLL for its tracking loop. The receiver hardware is nearly identical to the Mitel Architect, although the board layout is different. Differences include a real-time clock and non-volatile memory. The Orion receiver has flown in space aboard the student-designed experimental PC-Sat with preliminarily good results.<sup>7</sup> Detailed Orion receiver descriptions may be found in the technical report by Montenbruck, et. al.<sup>8</sup>

### PiVoT

The PiVoT (Position-Velocity-Time) receiver is produced by National Aeronautics and Space Administration's (NASA) Goddard Space Flight Center and is based on the GPS Builder architecture under a Linux environment and Plessey chipset. The PiVoT receiver is a single frequency design capable of outputting code and range rate measurements. It has four RF ports and two front end/correlators for planned attitude determination capability. The version that was tested did not have internal time tag synchronization to integer GPS seconds. A TCXO is used in the PiVoT. The source code was available and appeared to use a 2nd-order FLL tracking loop. The PiVoT receiver has no space flight history yet, as it was originally designed as a development tool for spaceborne GPS research.

### BlackJack

The BlackJack receiver is produced by NASA's Jet Propulsion Laboratory (JPL), based on the TurboRogue design. The test model was the ICESat (Ice, Cloud, and Land Elevation Satellite) Engineering Model on loan from NASA's Goddard Space Flight Center. The BlackJack receiver is a dual frequency, single RF design capable of outputting code and carrier phase measurements. The tests from this study

show code accuracy much better than normal Coarse Acquisition (C/A) code, so Precise (P) code or carrier smoothing of the C/A code measurement is assumed. It uses a steered VCXO to take code and carrier measurements, but does not internally correct time tags to integer GPS seconds. The firmware and tracking loops are proprietary to JPL, but there is a 10 second averaging period used to smooth the raw measurements. In addition, the BlackJack can track the Precise Code GPS signal even in the presence of anti-spoofing. Including the earlier TurboRogue receiver design the BlackJack has an extensive space flight history, with favorable results reported during use on Gravity Recovery and Climate Experiment (GRACE), Challenging Minisatellite Payload (CHAMP), Student Nitrous Oxide Explorer (SNOE), Shuttle Radar Topography Mission (SRTM), and Ocean Surface Topography Experiment (TOPEX/Poseidon).

### Force-19

The Force-19 receiver is produced by Trimble Navigation, Inc. It was modified by NASA Goddard Space Flight Center and Honeywell for use in the Space Integrated GPS/Internal Navigation (SIGI) sensor system. The test model is provided by NASA's Johnson Space Center (JSC). The Force-19 receiver is a single frequency design capable of outputting code and range rate measurements. Based on the accuracies observed in this test, it is assumed these measurements are carrier smoothed. It has four RF ports for attitude determination capability. The version tested did not have internal time tag synchronization to integer GPS seconds. A TCXO is used in the Force-19. The Force-19 receiver is currently in operation aboard the International Space Station (ISS) as part of the SIGI sensor system.

### Ship Channel

The Ship Channel receiver was designed and created at JSC as a dual RF receiver for navigation and heading estimation in the Houston ship channel. It is based on the same chipset as the Mitel Architect and Zarlink Orion receivers. The receiver is a 12 channel L1 only receiver and was tested with the same DLR source code as the Architect and Orion receivers. The receiver hardware is nearly identical to the Mitel Architect, with the main difference that the Ship Channel is dual RF capable.

### SGR-20

The SGR-20 receiver is produced by Surrey Satellite Technology Ltd. It is a 4 RF, 24 channel single frequency (L1) receiver. The receiver is space capable and has flown in space on the UoSat-12 and TMSat missions. Like other receivers in this study, the SGR-20 is also based on the Mitel chipset and the 2021 correlator. The tested model output code phase, accumulated carrier cycles, instantaneous phase, and shifted

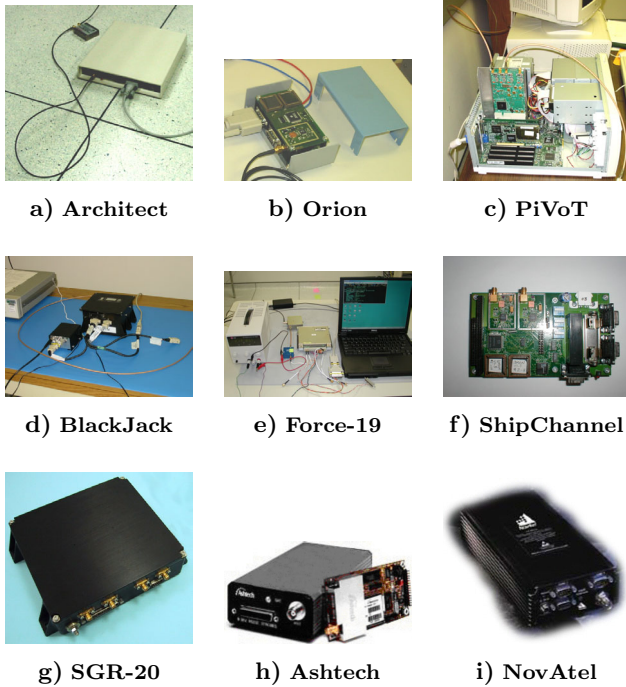


Fig. 3 GPS Receiver Test Sample

frequency. The code, carrier phase, and Doppler measurements had to be derived from the output of the SGR-20. Researchers at NASA/JSC had created a post-processing program for carrying out this operation.

#### Ashtech

The Ashtech G12 receiver is produced by Thales Navigation. The G12-HDMA OEM board was tested in this study. It is a single RF front-end receiver with 12 channels. The receiver outputs pseudorange, phase and Doppler at up to a 2 Hz rate. This receiver will be used in the Mini-AERCam satellite and has software modifications for space applications. All tracking loops and navigation algorithms are proprietary and could not be modified for this study.

#### NovAtel

The Millennium receiver is produced by NovAtel Inc. It is a 12 channel L1 and L2 GPS receiver. The receiver provides pseudorange, phase and Doppler measurements at both the L1 and L2 frequencies. The receiver is capable of generating the full P-code pseudorange measurement through proprietary cross-correlation techniques. A design feature for this receiver is NovAtel’s patented Narrow Correlator Technology. The technology allows the receiver to track pseudorange signals at a small chip width and thereby reduce the effects of multipath. All tracking loops and navigation algorithms are proprietary and could not be modified for this study.

## ANALYSIS

The analysis for this research is designed to produce performance results for low-level receiver measurements. Specifically, the analysis seeks to isolate raw measurement accuracy and systematic tracking loop errors. In a GPS measurement, however, the dominant features are the geometric quantities and oscillator errors. This research uses the technique of interchannel differencing to remove these errors. While Kaplan<sup>9</sup> mentions how this method has been used many times in relative positioning, its use in receiver performance analysis is a new development. In previous studies of raw measurement accuracy, curve fitting has been used to remove these errors.<sup>10</sup> While curve-fitting method does show the “white-noise” characteristics of the measurement, it has the disadvantage of masking any systematic errors in the receiver. These errors can identify otherwise undetected dynamic filter problems. By using differencing instead of curve-fitting, this study seeks to remove only the geometric and oscillator dependent errors and preserve the white-noise and systematic errors of the receiver. To effectively use this methodology, certain assumptions were made.

#### Assumptions

Some assumptions are made in the analysis to simplify the tests and processing. The main assumption concerns the reference truth measurements from the GPS constellation simulator. In a perfect test, the signal that is generated by the simulator is exactly what is output in the reference file. Since this is never entirely true, the results of the measurement differencing will actually give a combination of error from the receiver channels *and* the simulator. It is assumed for this procedure that the simulator error is negligible compared to the receiver error.

In addition, simulator truth estimates are collected at 1 second intervals and interpolated for receivers which do not output measurements with integer time tags. It is assumed that interpolation errors are negligible with respect to the measurements under analysis. To validate this, the simulated orbit is considered. For this scenario, the mean motion is approximately 1 mrad/s with accelerations  $\sim 8$  m/s<sup>2</sup>, acceleration rates  $\sim 20$  mm/s<sup>3</sup>, and fourth-order rates  $\sim 0.013$  mm/s<sup>4</sup>. A piecewise cubic Hermite polynomial interpolation method was used for which the error is well documented.<sup>11</sup> The error is represented as

$$\varepsilon(x) = f(x) - h_{2m-1}(x) = \psi_m(x)^2 \frac{f^{(2m)}(\xi)}{(2m)!} \quad (1)$$

where

$$\psi_m(x) = \prod_{j=0}^m (x - x_j)$$

$$f^k(\xi) = k^{\text{th}} \text{ deriv. of } f \text{ evaluated at } \xi$$

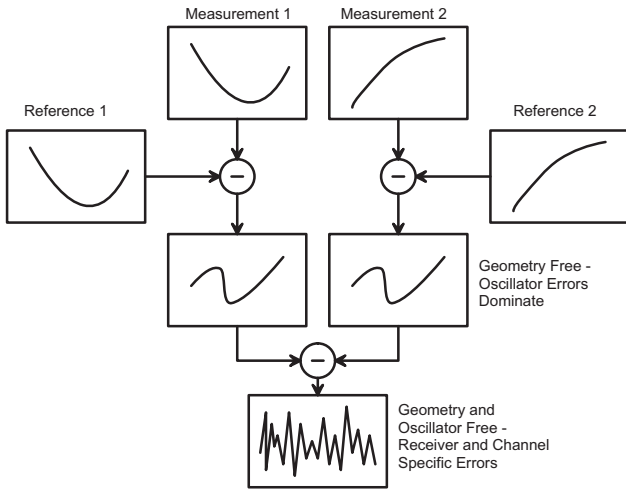


**Fig. 4 Measurement Differencing Technique**

and  $m=2$  for a cubic Hermite polynomial. By selecting the nearest time interval so that the interpolation is always less than  $\frac{1}{2}$  second, the neglected term represents less than  $4 \times 10^{-5}$  mm, which is many orders of magnitude smaller than the most accurate carrier phase measurement in the test.

Finally, the simulated signal levels are assumed to be the actual signal levels experienced in an orbital environment. This is important because tracking loop performance can be directly affected by low Signal-to-Noise Ratio (SNR). While simulated signal levels will vary with preamplifier and front-end selection, a common power level was selected as +8 dB above the nominal GPS signal level. The power increase is detailed as follows:

- +3 dB: Average antenna gain
- +3 dB: GPS signal level higher than published
- +2 dB: Thermal noise floor is higher in electronic simulator than in real environment - need higher signal level to maintain same SNR

This power level gives SNR readings in most receivers which are similar to live-sky tests.

#### Differencing

Figure 4 shows the analysis technique used for the tests. As stated before, the dominant features of a receiver measurement are the geometric distance (range) and speed (range rate) between the receiver and GPS satellite. The first step in the data analysis is to subtract the simulated, reference geometric quantities from the measurement to give an “error from truth” representation. This is analogous to the classic GPS “receiver-receiver” single-difference technique except the simulated reference is used as one of the “receivers.” The quantity that results is free from common-mode satellite errors and is dominated by receiver oscillator drifts and other errors. This procedure is performed for two GPS measurements at a time when their visibility overlaps. Mathematically, the receiver measurement,  $Meas_i$ , consists of range,

$\rho_i$ , oscillator errors,  $\delta T$ , and other receiver errors,  $\epsilon_i$ .

$$Meas_i = \rho_i + \delta T + \epsilon_i \quad (2)$$

The simulator reference,  $Ref_i$ , consists of range,  $\rho_i$ , and simulator errors,  $\epsilon_{Si}$ .

$$Ref_i = \rho_i + \epsilon_{Si} \quad (3)$$

These are subtracted to give the single difference,  $SD_i$ .

$$\begin{aligned} SD_i &= Meas_i - Ref_i \\ &= \delta T + \epsilon_i + \epsilon_{Si} \end{aligned} \quad (4)$$

The next step in the analysis is to difference the results of the previous operations on two different measurements taken at the same time. This removes common oscillator errors and the remaining quantity represents receiver and channel specific errors. This is analogous to the classic GPS double-difference except the result is not a baseline between two receivers but an error measurement of a single receiver. This result is the double difference,  $DD_{1-2}$ .

$$\begin{aligned} DD_{1-2} &= SD_1 - SD_2 \\ &= +\epsilon_1 - \epsilon_2 + \epsilon_{S1} - \epsilon_{S2} \end{aligned} \quad (5)$$

As stated previously, it is assumed the last two terms (simulator errors) are negligible with respect to the first two (receiver/channel specific errors). If the errors are independent and have equal standard deviation, the resulting Root Mean Square (RMS) error will be scaled by  $\sqrt{2}$  since a double difference was used. For these independent errors, the receiver intrinsic accuracy,  $Acc(\epsilon)$ , is related to the measured error,  $\epsilon_{meas}$ , as discussed in Yates:<sup>12</sup>

$$\begin{aligned} Acc(\epsilon_{meas}) &= \sqrt{\frac{1}{n} \sum_{i=1}^n \epsilon_i^2} \\ RMS(\epsilon_{meas}) &= \sqrt{\frac{1}{n} \sum_{i=1}^n 2\epsilon_i^2} \\ &= \sqrt{2}Acc(\epsilon_{meas}) \end{aligned} \quad (6)$$

The reported accuracy will be a mean value of all errors from both channels and the simulator.

#### Data Arc Selection

Receiver performance may be characterized in terms of application specific parameters (e.g., multipath) and application independent parameters (e.g., tracking loop error). In order to create a general measurement of receiver performance, application independent parameters were evaluated. These parameters are believed to be functions of signal dynamics (Doppler shift) and signal strength (SNR).

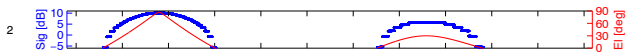
To examine receiver performance in a variety of conditions, six data arcs were selected from the simulation

**Table 1 Dynamics and Signal Level Conditions**

PRN 1	PRN 2	Start Time (sec)	End Time (sec)	Max Signal Level (dB)	Max Relative Acceleration (g's)
2	28	174000	175800	10	0.1
14	29	178100	180000	9	0.2
3	15	177400	178900	8	0.3
21	28	173900	174700	9	0.9
13	22	176500	177700	9	1.0
6	17	177100	178000	7	0.8

at standardized time intervals. Since satellite selection algorithms vary from receiver to receiver, no guarantee exists that a receiver will track both satellites during a particular test interval. With six test intervals, however, most receivers will provide consistent data for at least some of the intervals. In this entire study, in fact, there were relatively few instances among the nine receivers where a data arc was unusable due to satellite non-selection.

These data arcs contain a variety of relative dynamics and signal level conditions. This is important because, as discussed, the raw measurement accuracy is affected by these two factors. The relative dynamics conditions come from the differential velocity and acceleration of the two GPS satellites. Satellites with similar rise/set profiles will have low relative dynamics whereas satellites with differing rise/set profiles will have high relative dynamics. The highest relative dynamics will occur when one SV is just rising (or setting) as the other reaches the peak of its arc. The highest signal levels will occur when both satellites have high elevations at the same time. Table 1 summarizes the relative dynamics and signal level conditions for the standardized test intervals. Figure 5 shows sample rise/set profiles for the GPS satellites visible in the simulation. The solid red line represents the local elevation in degrees, while the blue points represent the signal level in decibels (dB). These plots were used to select the standard test intervals based on common satellite visibility and line-of-sight (LOS) acceleration.

**Fig. 5 Sample GPS Satellite Arc for Test Scenario**

## RESULTS

This section presents the results of the polar, on-orbit benchmark test. The measured accuracy is discussed for each receiver and sample plots are shown for notable results. Comprehensive plots for many of the receivers may be found in Holt.<sup>13</sup> Results are listed as “N/A” (Not Available) when the receiver does not output a particular type of measurement or did not track one of the specified satellites during the run. All accuracy assessments are presented together in Table 2 at the beginning of the section for convenient comparison. This table also gives the average results for

each receiver and measurement type. Any processing abnormalities or identifiable sources of error are detailed at the beginning of the section for a particular receiver.

A particularly interesting set of results comes from the Architect, Orion, and Ship Channel receivers. These receivers were tested using the same firmware version, so all differences in performance should be attributable to hardware and board layout. This is a unique opportunity to examine exactly how these factors affect the GPS raw measurement. As the results will show, the performance of these three receivers is nearly identical.

In all of the results, it is important to notice any systematic errors. These errors can be observed by using the differencing technique employed in this study. In several cases (Orion, Force-19), the systematic error results were actually used for debugging to correct tracking loop or time tag errors. In the case of the Force-19 pseudorange performance, the measurement errors are larger than reported in Table 2 if systematic errors are included.

### Architect

The Mitel Architect was tested with the same source code build as the Zarlink Orion. The code version was ‘DLR16707H’ developed by GSOC.<sup>8</sup> Any differences should therefore be related to board layout or component disparities. The pseudorange output is smoothing capable, but for this test only unsmoothed pseudorange was considered.

It is clear in Figure 6(a) that the Architect receiver in this test configuration has no systematic errors in pseudorange, carrier phase, or range rate measurements. The noise is in an expected range for unsmoothed values of pseudorange and range rate. Since the Architect uses the same hardware and code version as the Orion, it was expected that these two receivers would produce similar results. When the Architect result is compared with the Orion result in Figure 6(b), this is found to be the case.

### Orion

The Zarlink Orion was tested with the same source code build as the Mitel Architect. The code was ‘DLR16707H’ developed by GSOC. Any differences in performance should therefore be related to board layout or component disparities. The pseudorange output is smoothing capable, but for this test only code-based pseudorange was considered.

In early tests with this receiver, a systematic trend was found in the carrier phase measurements. The same trend was found in the Mitel Architect, so a hardware disparity issue was ruled out. This trend is shown in Figure 6(b), with the original in red and the corrected in blue. The trend appears to be proportional to the LOS accelerations shown in Table 1, a result consistent with the use of the second order

**Table 2 Receiver Accuracy Assessment Results**

PR = Pseudorange, CP = Carrier Phase, RR = Range Rate

		Receiver									
		Architect	Orion	PiVoT	BlackJack	Force-19	Ship Ch.	SGR-20	Ashtech	NovAtel	
2-28	PR Error [m]	0.9258	0.9477	1.0368	0.1553	0.0151	0.8145	N/A	0.5390	0.0991	
	CP Error [mm]	0.9323	0.9253	N/A	0.5033	~2.597	1.4337	N/A	3.1626	1.1970	
	RR Error [m/s]	0.1407	0.1414	0.2400	~0.001	0.0110	0.1050	N/A	0.0808	0.0745	
14-29	PR Error [m]	0.9037	0.9193	1.1267	0.1025	0.0324	N/A	N/A	0.5244	0.1121	
	CP Error [mm]	0.9227	1.0890	N/A	0.4227	~2.717	N/A	N/A	3.2377	1.2567	
	RR Error [m/s]	0.1382	0.1440	0.2097	~0.001	0.0116	N/A	N/A	0.0787	0.0359	
3-15	PR Error [m]	0.9015	0.9559	1.5009	0.1323	0.0145	N/A	1.3810	0.6362	0.1226	
	CP Error [mm]	1.0899	1.0699	N/A	0.4105	~2.923	N/A	N/A	3.5167	1.3715	
	RR Error [m/s]	0.1419	0.1561	0.4381	~0.001	0.0124	N/A	0.1858	0.0876	0.0351	
21-28	PR Error [m]	0.9131	0.9029	N/A	0.1539	0.0101	0.8244	N/A	0.5996	0.1267	
	CP Error [mm]	1.1566	1.6478	N/A	0.9524	~3.250	2.1160	N/A	3.5311	1.3559	
	RR Error [m/s]	0.1526	0.1512	N/A	~0.001	0.0138	0.1136	N/A	0.0869	0.0426	
13-22	PR Error [m]	0.8986	0.8960	1.2179	0.1606	0.0100	N/A	1.4248	0.6092	0.1217	
	CP Error [mm]	1.1864	1.7767	N/A	0.6380	~3.102	N/A	N/A	3.5580	1.3480	
	RR Error [m/s]	0.1469	0.1473	0.4074	~0.001	0.0132	N/A	0.1221	0.0890	0.0565	
6-17	PR Error [m]	0.9297	0.8942	1.2229	0.1242	0.0129	N/A	1.3693	0.6598	0.1285	
	CP Error [mm]	1.2112	1.5659	N/A	0.2833	~3.399	N/A	N/A	3.8485	1.4228	
	RR Error [m/s]	0.1466	0.1534	0.2799	~0.001	0.0144	N/A	0.1283	0.0997	0.0401	
Overall	PR Error [m]	0.9121	0.9193	1.2210	0.1381	0.0158	0.8194	1.3917	0.5947	0.1184	
	CP Error [mm]	1.0831	1.3458	N/A	0.5350	N/A	1.7749	N/A	3.4758	1.3253	
	RR Error [m/s]	0.1445	0.1489	0.3150	N/A	0.0127	0.1093	0.1454	0.0871	0.0475	
						P-code Capable	Carrier Smoothed				P-code Capable

PLL found in the Orion. This information was used in code debugging to internally correct the carrier phase measurements for acceleration dependence by numerically estimating the acceleration. A third order PLL is also under development to remove the acceleration. It is significant to note that only this differencing test could identify a systematic trend and allow for the relatively simple correction.

With the corrected code it is clear that the Orion receiver in this test configuration has no systematic errors in pseudorange, carrier phase, or range rate measurements. The noise is in an expected range for unsmoothed values of pseudorange and range rate. Again, since the Orion uses the same hardware and code version as the Architect, it was expected that these two receivers would produce similar results (see Figure 6(a)).

PiVoT

The PiVoT receiver was tested with code build “GPS BUILDER A-1.3” provided by the NASA Goddard Space Flight Center.<sup>14</sup> It outputs code and range rate measurements only, not currently possessing the capability to make carrier phase measurements. This code, therefore, does not use carrier smoothing in the pseudorange or range rate measurements.

In the low relative dynamics case shown in Figure 6(c), the results show expected noise values and a small systematic “wobble” in the range rate. A high relative dynamics case had an expected increase in noise.

In addition, the pseudorange measurements showed a small systematic trend at the beginning and end of the test interval (corresponding to low SNR levels) and the range rate measurements show fairly large outliers. These outliers seem to follow a systematic downward slope for the duration of the test interval. This phenomena appears in all the PiVoT tests with high LOS accelerations.

BlackJack

The BlackJack receiver was tested with the ICE-Sat code build provided by NASA’s Jet Propulsion Laboratory. The BlackJack receiver hardware was the ICESat Engineering Model flight spare unit.

The BlackJack receiver had some anomalies which made processing difficult. Most of these were from known receiver issues which have been addressed by JPL. Most prominent among these was the unexpected loss of Coarse Acquisition (C/A) code tracking for some high elevation satellites which causes a subsequent drift error in the carrier phase measurements. For this study, the lost-lock measurements were not considered as they would have severely altered the statistics of the correct measurements.

Although range-rate measurements are not output directly by the receiver, their accuracy can be estimated from the carrier phase measurements by assuming a sample rate of 1 Hertz:

$$Acc_{RR} \approx \sqrt{2} Acc_{CP} / dT \tag{7}$$

For independent sequential errors, the factor of  $\sqrt{2}$  is



introduced by differencing the carrier measurements to give the range rate. Systematic trends will not follow this pattern as the errors are correlated with time.

The BlackJack receiver uses proprietary smoothing algorithms developed by JPL. These algorithms limit data output to 10 second intervals, as opposed to the 1 second interval used in the other tested receivers. The unsmoothed code and range rate measurements are not available for output. For low dynamics cases, noise levels are lower than most of the other tested receivers. This is expected from a highly smoothed solution. The receiver experienced the previously discussed data dropouts during all the runs. Figure 6(d) shows a high dynamics case where the noise is slightly higher as expected. Surprisingly, however, a systematic drift occurs in the carrier phase measurement. Whether this is a hardware error or a tracking loop error is currently under investigation by JPL.

#### Force-19

The Force-19 receiver was tested using code build 1.10 with attitude code S5.04 supplied by NASA’s Johnson Space Center.

The Force-19 receiver had some notable time tagging difficulties discovered by this test which hindered data processing. The pseudorange and range rate measurements both seemed to be reported with time tags that were not consistent with true GPS time. As stated earlier, one important feature of this testing method is the ability to see systematic drifts that would be masked by conventional curve fitting. This advantage was displayed prominently in the Force-19 test. In all the range rate results, a systematic error was seen which was proportional to the LOS acceleration of the test. Upon closer inspection, a 1/6 second time tag offset was found relative to GPS time. This would be consistent with a range rate calculated by a central difference derivative of the carrier phase measurement at a 3 Hertz carrier sample rate. Half of this sample interval is 1/6 second, and when the correction is applied to the time tag the systematic trend is removed as shown in Figure 6(e). Pseudorange observations also seem to have a time tag error with the same curvature as the line-of-sight velocity but no consistent offset has been found as of this writing. Application of the receiver reported clock bias to the time tag does not appear to correct this problem.

Although the receiver does not directly output absolute carrier phase measurements, the carrier phase is used to smooth the code measurements and derive the range rate. From the carrier-derived range rate accuracy, the carrier phase accuracy can be estimated by

$$\begin{aligned} Acc_{CP} &\approx Acc_{RR}(dT)/(\sqrt{2}) & (8) \\ Acc_{CP} &\approx Acc_{RR}/(3\sqrt{2}) \end{aligned}$$

where the factor of  $\sqrt{2}$  comes from the carrier phase

derivative and the factor of 3 comes from the 3 Hertz carrier sample rate found in the receiver.

Figure 6(e) shows the apparent time tag error discovered in this test. The red curve represents the uncorrected measurement, while the blue curve shows the result with a 1/6 second correction applied. The typical results showed expected noise levels for carrier smoothed code and carrier-derived range rate results. The systematic drift is very apparent in the pseudorange, with another time tag error as a possible cause.

#### Ship Channel

The Ship Channel was tested with the same source code as the Zarlink Orion. The code was ‘DLR16707H’ developed by GSOC. Any differences should therefore be related to board layout or component disparities. The pseudorange output is smoothing capable, but for this test only code-based pseudorange was considered.

It is clear in Figure 6(f) that the Ship Channel receiver in this test configuration has no systematic errors in pseudorange, carrier phase, or range rate measurements. The noise is in the expected range for unsmoothed values of pseudorange and range rate. Since the Ship Channel uses the same hardware and code version as the Orion, it was expected that these two receivers would produce similar results. When the Ship Channel result is compared with the Orion result in Figure 6(b) this is found to be the case.

#### SGR-20

The SGR-20 receiver was tested with the code build supplied by the manufacturer. It outputs code, carrier, and range rate measurements, although the carrier output is anomalous. This code does not use carrier aiding in the pseudorange or range rate measurements.

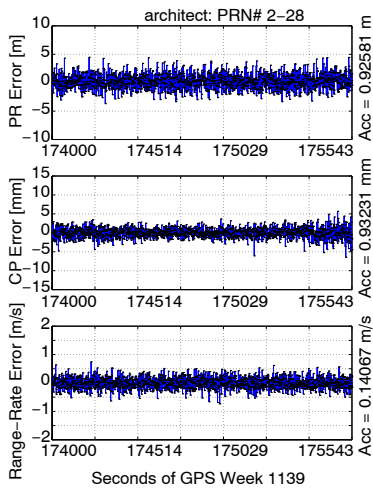
From inspection of the carrier measurements, it appears that the phase-lock-loop was not operating properly. The code build was proprietary and not available, so no direct examination or repair was possible. For this test, therefore, the carrier measurement was not usable. In addition, the receiver had many periods of lost signal lock that hindered the test.

In low relative dynamics cases, the results show expected noise values but large periods of signal loss. For high relative dynamics cases there was an expected increase in pseudorange noise. Again, carrier phase measurements were unusable for the tests conducted on this receiver.

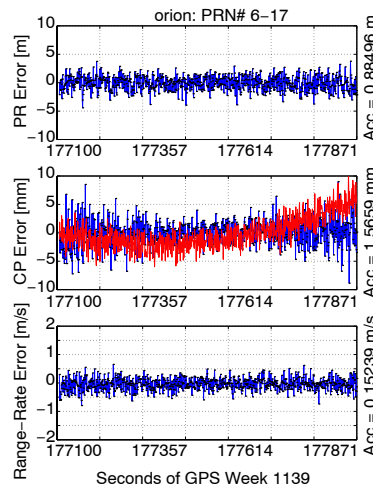
#### Ashtech

The Ashtech G12 was tested with proprietary source code provided by the manufacturer. It outputs code, carrier, and range rate measurements at a frequency of 1 Hz.

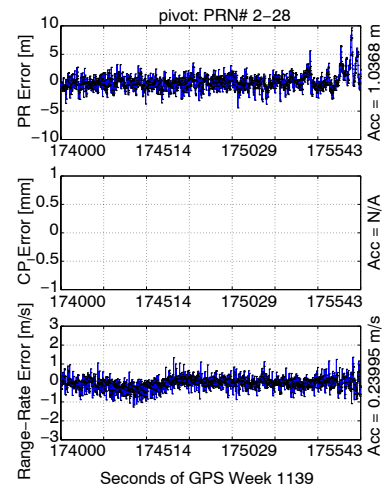
For low dynamics cases, noise levels are as expected. It is clear that the Ashtech receiver in this test configuration has no systematic errors in pseudorange, carrier phase, or range rate measurements. Figure 6(h) shows



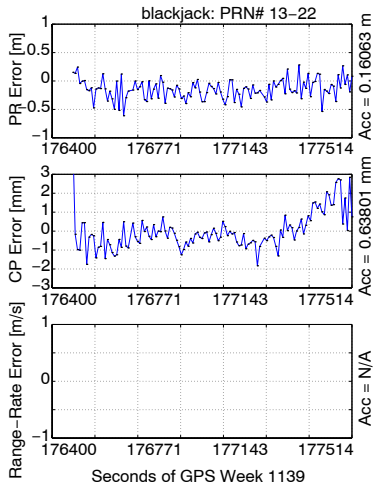
a) Architect Low Dynamics



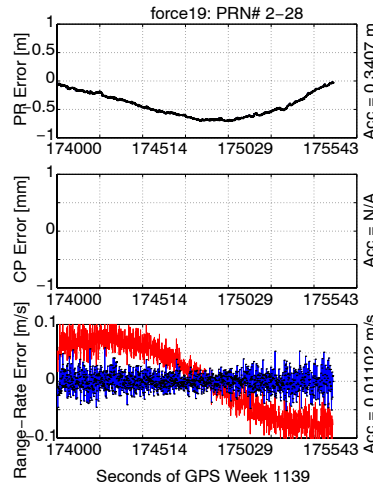
b) Orion Systematic Acceleration Dependence Before (red) and After (blue) Tracking Loop Modifications



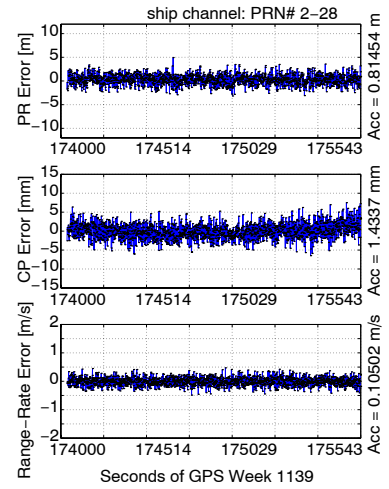
c) PiVoT Low Dynamics



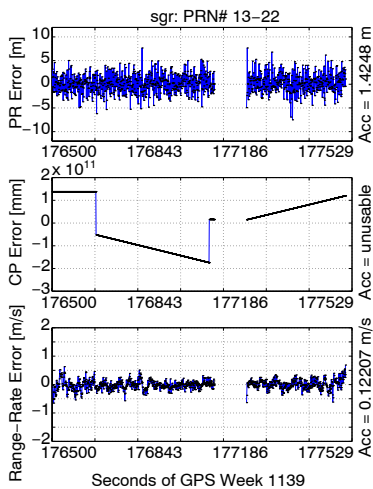
d) BlackJack High Dynamics



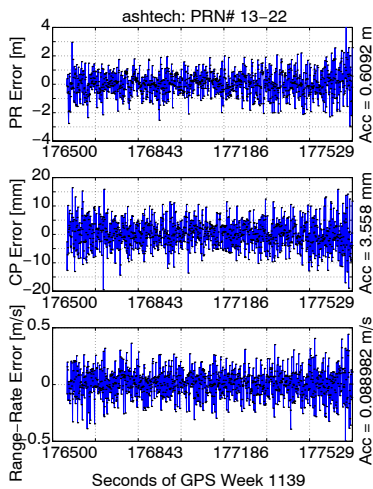
e) Force-19 Range Rate Time Tag Error Without (red) and With (blue) Time Tag Correction



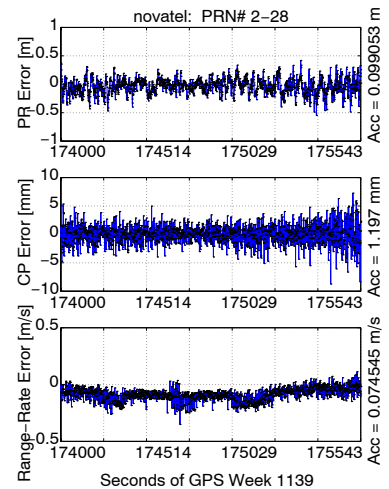
f) Ship Channel Low Dynamics



g) SGR-20 High Dynamics



h) Ashtech High Dynamics



i) NovAtel Low Dynamics

Fig. 6 Force-19, Ship Channel, Ashtech, and NovAtel Receiver Result

a high dynamics case where the noise is slightly higher as expected. The Ashtech range-rate measurements were the most accurate of any receiver tested, even those with P-code and smoothing capabilities.

#### NovAtel

The NovAtel receiver was tested with proprietary source code supplied by the manufacturer. It outputs code, carrier, and range rate measurements at a frequency of 1 Hz. The receiver is P-code capable, so it was tested with a P-code included in the simulated signal. The accuracy reflects the expected improvements from this ability.

A low dynamics case is shown in Figure 6(i), where noise levels are among the lowest of all tested receivers. This is expected from a P-code capable receiver. It is clear that the NovAtel receiver in this test configuration has no systematic errors in pseudorange, carrier phase, or range rate measurements. For high dynamics cases the noise is slightly higher as expected. The NovAtel results were among the best of all receivers tested in this study, with no signal losses or dropouts encountered during the testing.

### CONCLUSIONS

Although the original motivation for this research was to allow mission designers to compare receiver performance, the utility of the results in enabling receiver designers to improve their product's performance has also been demonstrated. The test results and methods presented in this study have already contributed to improvements in several receiver designs. Because raw accuracy and systematic errors can both be observed, the potential for debugging receivers is improved over traditional RMS noise methods. The simulated high Doppler environment also allows a more realistic evaluation of LOS acceleration dependencies. This research not only provides receiver designers with an important debugging tool but also provides mission planners with an independent evaluation of raw measurement accuracy and tracking loop performance. This is a significant improvement over manufacturer supplied specifications that are usually "best-case" results with little or no mention of tracking loop performance.

This research focused on the low-level measurement accuracy of a GPS receiver. The ultimate navigation solution produced by a system will depend heavily on estimation algorithms and filtering techniques that are not evaluated here. All of these systems, however, are based on the common raw measurements that a receiver must make to perform navigation. If problems in the raw measurement quality are identified and repaired, the ultimate navigation solution will improve as well. For example, the Orion and Architect receiver tests gave carrier phase measurements which showed an acceleration dependence. Only a differencing test would preserve this systematic error in the results. A fairly simple firmware adjustment led to

a large improvement in the raw measurement quality. The Force-19 time tag error is another example of the type of raw measurement improvement which this study made possible. Any tracking loop error which is identified and repaired using these tests will ultimately improve the overall navigation ability of the GPS receiver.

It is hoped that this research will increase the knowledge and usage of benchmark testing among the GPS design community. This study demonstrates that independent evaluations are important for complex embedded systems such as GPS receivers. Spacecraft missions costing millions of dollars can be marginalized or rendered ineffective by a poorly performing GPS receiver. The need for independent testing and debugging will only increase as GPS becomes a standard system for spacecraft navigation. This research shows that substantive improvements in receiver performance can be obtained by accurately testing the receiver's measurements. Using these improvements, better spacecraft mission performance can be obtained without significantly increasing the mission cost.

### REFERENCES

- <sup>1</sup>Montenbruck, O., G. Holt, "Spaceborne GPS Receiver Performance Testing," Tech. Rep. TN 02-04, DLR, Oberpfaffenhofen, 2002.
- <sup>2</sup>Williams, J., et. al., "Testing of the ICESat BlackJack GPS Receiver Engineering Model," *Proceedings of ION GPS Conference*, Portland, OR, September 2002.
- <sup>3</sup>Stone, J. et. al., "GPS Pseudolite Transceivers and Their Applications," *Presented at the ION National Technical Meeting 99*, January 1999.
- <sup>4</sup>"STR Series Multichannel Satellite Navigation Simulators Reference Manual," Tech. Rep. DGP00032AAC, Spirent Communications, Ltd., Devon, UK, 2001.
- <sup>5</sup>Holt, G., "GPS Receiver Benchmark Testing," Tech. rep., The University Of Texas Center for Space Research, Austin, TX, March 2002.
- <sup>6</sup>"GPS Architect Users Guide," Tech. Rep. DM4921, Mitel Semiconductor, Wiltshire, UK, March 1997.
- <sup>7</sup>Montenbruck, O., et. al., "GPS Operations on the PCsat Microsatellite," *Proceedings of ION GPS Conference*, Portland, OR, September 2002.
- <sup>8</sup>Montenbruck, O., M. Markgraf, and S. Leung, "Space Adaptation of the GPS Orion Firmware," Tech. Rep. DLR/GSOC TN 01-08, Oberpfaffenhofen, November 2001.
- <sup>9</sup>Kaplan, E., ed., *Understanding GPS Principles and Applications*, Artech House, Boston, 1996.
- <sup>10</sup>Ryan, S., et. al., "DGPS Kinematic Carrier Phase Signal Simulation Analysis in the Velocity Domain," *Proceedings of ION GPS Conference*, Kansas City, MO, September 1997.
- <sup>11</sup>Atkinson, K., *An Introduction to Numerical Analysis*, Wiley, New York, 1978.
- <sup>12</sup>Yates, R., D. Goodman, *Probability and Stochastic Processes*, John Wiley and Sons, New York, 1999.
- <sup>13</sup>Holt, G., *Benchmark Testing for Spaceborne Global Positioning System Receivers*, Thesis, The University of Texas at Austin, 2002.
- <sup>14</sup>Cecchini, J., et. al., "SIGI SP Interface Control Document to Trimble GPS Receiver with Goddard Space Flight Center Attitude Microprocessor Software," Tech. Rep. ICD 34204012, Honeywell Sensor and Guidance Products, Clearwater, FL, May 1998.